Radiation-induced reduction–polymerization route for the synthesis of PEDOT conducting polymers

Zhenpeng Cui [a], Cecilia Coletta [a], Rolando Rebois [a], Sarah Baiz [b], Matthieu Gervais [b], Fabrice Goubard [c], Pierre-Henri Aubert [c], Alexandre Dazzi [a], Samy Remita [a,d,*]

[a] Laboratoire de Chimie Physique, LCP, UMR 8000, CNRS, Université Paris-Sud 11, Bât.349, Campus d'Orsay, 15 avenue Jean Perrin, 91405 Orsay Cedex, France
[b] Laboratoire Procédés et Ingénierie en Mécanique et Matériaux, PIMM, ENSAM, UMR 8006, CNRS, CNAM, 151 boulevard de l'hôpital, 75013 Paris, France
[c] Laboratoire de Physicochimie des Polymères et Interfaces, LPPI, EA 2528, Université de Cergy-Pontoise, 5 mail Gay Lussac, Neuville sur Oise, 95031 Cergy-Pontoise Cedex, France
[d] Département CASER, Ecole SITI, Conservatoire National des Arts et Métiers, CNAM, 292 rue Saint-Martin, 75141 Paris Cedex 03, France

HIGHLIGHTS

- A reduction–polymerization route is developed for synthesizing conducting polymers.
- Hydrated electrons are used to reduce EDOT monomers into PEDOT polymers.
- A mechanistic study of EDOT reduction is considered.
- Chemical and morphological characterizations of PEDOT are made.
- Their properties are compared with those of PEDOT polymers previously synthesized.

GRAPHICAL ABSTRACT

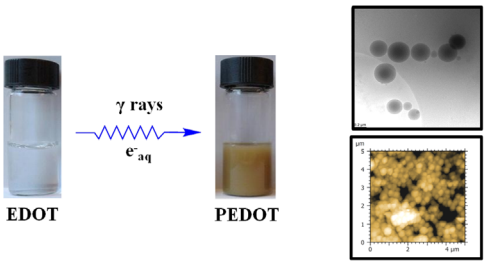

ABSTRACT

Synthesis of conducting poly(3,4-ethylenedioxythiophene), PEDOT, is achieved through an original reduction–polymerization route: γ-radiolysis of aqueous solutions containing EDOT monomers under N_2 atmosphere. According to UV–vis absorption spectrophotometry and ATR-FTIR spectroscopy, reduction of EDOT is initiated by hydrated electrons produced by water radiolysis and leads to PEDOT polymers through coupling reactions. The morphology of PEDOT is characterized by Cryo- TEM microscopy in aqueous solution and by SEM after deposition. In an original way, high resolution AFM microscopy, coupled with infrared nanospectroscopy, is used to probe the local chemical composition of PEDOT nanostructures. The results demonstrate that spherical self-assembled PEDOT nanostructures are formed. TGA analysis and four point probe measurements demonstrate that thermal stability and electrical conductivity of PEDOT polymers obtained by the present original reduction–polymerization method are close to those of PEDOT we previously prepared by radiolysis according to an oxidation–polymerization route.

Keywords:
Radiolysis
Conducting polymers
PEDOT
Reduction–polymerization

1. Introduction

Conducting polymers (CP), as a unique class of π-conjugated materials, received great interests due to their potential technological applications as organic semi-conducting materials for the fabrication of sophisticated electronic devices such as field-effect transistors, electroluminescent diodes, chemical or biological

* Corresponding author at: Laboratoire de Chimie Physique, LCP, UMR 8000, CNRS, Université Paris-Sud 11, Bât.349, Campus d'Orsay, 15 avenue Jean Perrin, 91405 Orsay Cedex, France.
E-mail address: samy.remita@u-psud.fr (S. Remita).

sensors and photovoltaic cells (Heeger, 2001; Cho et al., 2014; Ghosh et al., 2015; Balint et al., 2014; Adeloju and Wallace, 1996; Jang et al., 2005; Patil et al., 1988; Abdelhamid et al., 2015).

Among the most renowned CP, poly(3,4-ethylenedioxythiophene) polymers (PEDOT, Scheme 1) were mostly investigated for their easy synthesis, good environmental stability and high electrical conductivity (Roncali et al., 2005; Wang, 2009; Kirchmeyer and Reuter, 2005).

In literature, PEDOT is usually synthesized by oxidation–polymerization routes thanks to the initial oxidation of 3,4-ethylenedioxythiophene monomers (EDOT, Scheme 1) and to the further coupling reactions in α,α′ positions. In fact, due to their strong electron donor effect, the ether groups at the β, β′ positions of thiophene rings, which confer a high reactivity to the free α, α′ positions, prevent the formation of parasite $\alpha-\beta'$ linkages during polymerization.

While the more traditional oxidation–polymerization ways consist in chemical or electrochemical methods (Jiang et al., 2012; Baik et al., 2009; Li et al., 2009), some alternative approaches such as vapor-phase and enzyme-catalyzed polymerization are also reported (Lawal and Wallace, 2014; Atanasov et al., 2014; Rumbau et al., 2007).

In our previous work, an easy and "green" methodology was developed by using γ-rays to induce oxidation–polymerization of EDOT in aqueous solution at air (Lattach et al., 2013). Also, by adjusting polymerization conditions, different oxidizing species, namely hydroxyl and azide radicals, were produced under N_2O atmosphere by γ-radiolysis leading to self-assembled PEDOT nanostructures with different morphologies (Lattach et al., 2014). More recently, the work was extended to other kinds of CP since oxidation–polymerization of pyrrole (Py) monomers was achieved leading to spherical and chaplet-like polypyrrole (PPy) nanostructures (Cui et al., 2014). Therefore, radiolytic methodology, especially γ-irradiation, has definitely proved to be a useful alternative approach for the oxidation–polymerization of nanostructured CP. Nevertheless, to the best of our knowledge, radiation chemistry has never been used, in reducing conditions, as a route for conducting polymers reduction–polymerization.

In this work, starting from monomers dissolved in water, we describe for the first time a simple γ-rays-based reduction–polymerization route for synthesizing conducting polymers under N_2 at room temperature. The originality of the work comes from the use, during the initiation step of polymerization, of reducing species produced from water radiolysis, namely hydrated electrons (e^-_{aq}), instead of oxidizing radicals, such as hydroxyl radicals ($HO^\cdot$). Morphology and physicochemical properties of PEDOT synthesized by reduction–polymerization (action of e^-_{aq} under N_2 atmosphere), noted **$PEDOT_{red}$**, are checked and compared with those of PEDOT already synthesized by γ-irradiation under oxidative conditions, noted **$PEDOT_{ox}$** (action of $HO^\cdot$ under N_2O atmosphere).

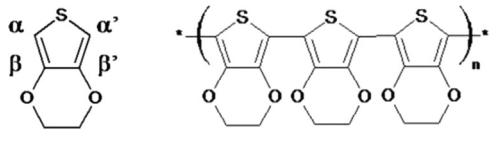

Scheme 1. Chemical structures of 3,4-ethylenedioxythiophene (EDOT) and poly (3,4-ethylenedioxythiophene) (PEDOT). EDOT structure displays the free α, α′ positions where polymerization could occur.

2. Materials and methods

2.1. Chemical reagents

3, 4-ethylenedioxythiophene (EDOT) (≥98%, Sigma-Aldrich) was used as the monomer and ultrapure water (Millipore system, 18.2 MΩ cm) was used as solvent. N_2O and N_2 (Air Liquid Co.) were used to degas aqueous solutions in order to prepare $PEDOT_{ox}$ and $PEDOT_{red}$ respectively. For $PEDOT_{red}$ synthesis, isopropanol (≥99.5%, Sigma-Aldrich), as hydroxyl radicals scavenger, was used without any treatment. Nitrosyl tetrafluoroborate ($NOBF_4$) (≥95%, Sigma-Aldrich) dissolved in acetonitrile (≥99.9%, Sigma-Aldrich) was used as dopant during the electrical conductivity measurements.

2.2. Water radiolysis and radiation-induced polymerization

It is well known that γ-irradiation of deoxygenated diluted aqueous solutions (under N_2 for instance) at neutral pH produces the following species within nanosecond timescale (Spinks and Woods, 1990; Ferradini and Jay-Gerin, 2000, 1999):

$$H_20 \rightarrow HO^\cdot + H^\cdot + e^-_{aq} + H_3O^+ + H_2O_2 + H_2 \quad (1)$$

Under such experimental conditions, radiolytic yields (*G*-values) of hydroxyl radical ($HO^\cdot$) and hydrated electron (e^-_{aq}) are well-known (Spinks and Woods, 1990; Ferradini and Jay-Gerin, 2000):

$$G_{HO^\cdot} = 2.8 \times 10^{-7} \text{ mol J}^{-1} \quad (2)$$

$$G_{e^-_{aq}} = 2.8 \times 10^{-7} \text{ mol J}^{-1} \quad (3)$$

The relatively low production yield (0.6×10^{-7} mol J^{-1}) of hydrogen atoms, $H^\cdot$, enables us to neglect their presence in the irradiated medium. $HO^\cdot$ radicals are strong oxidative species with a redox potential that amounts to $E^0_{ESH}(HO^\cdot/H_2O) = 2.3\ V_{ESH}$ at pH 7, while hydrated electrons, e^-_{aq}, are very reducing species ($-2.8\ V_{ESH}$) (Hart, 1969). Due to these two extremal redox potential values, one can consider the possible oxidation of EDOT ($1.4\ V_{Ag/AgCl}$) by hydroxyl radicals and its possible reduction by hydrated electrons.

In order to reduce EDOT and then to synthesize $PEDOT_{red}$, hydroxyl radicals must be scavenged. This is possible, under N_2 atmosphere, in the presence of isopropanol, $(CH_3)_2CHOH$. Indeed, when isopropanol is present (at a relatively high concentration, 0.2 mol L^{-1} for instance), $HO^\cdot$ is quantitatively converted into isopropanol radical, $(CH_3)_2C\cdot OH$, (Song et al., 2007; Belloni et al., 1998) according to:

$$(CH_3)_2CHOH + HO^\cdot \rightarrow (CH_3)_2C\cdot OH + H_2O \quad (4)$$

Note that isopropanol radical cannot oxidize EDOT. In fact, it is almost a reducing species, the redox potential of which amounts to $-1.8\ V_{ESH}$ at pH = 7. As a consequence, when irradiating N_2-saturated aqueous solutions in the presence of isopropanol, as in the case of our EDOT solutions, in addition to hydrated electrons ($G_{e^-_{aq}} = 2.8 \times 10^{-7}$ mol J^{-1}), only an additional short-lived transient species is quantitatively formed, namely isopropanol radicals, the radiolytic yield of which being:

$$G\left((CH_3)_2C\cdot OH\right) = G_{HO^\cdot} = 2.8 \times 10^{-7} \text{ mol J}^{-1} \quad (5)$$

On the contrary, in order to oxidize EDOT and then to synthesize $PEDOT_{ox}$, hydrated electrons must be scavenged. This is possible under N_2O atmosphere. Indeed, when the aqueous solution is saturated with nitrous oxide (25 mM in N_2O) instead of N_2, e^-_{aq} is quantitatively consumed and produces $HO^\cdot$ radicals (Spinks and

Woods, 1990) according to:

$$e^-_{aq} + N_2O + H_2O \rightarrow HO\cdot + HO^- + N_2 \quad (6)$$

As a consequence, when irradiating N_2O-saturated aqueous solutions at neutral pH, as in the case of EDOT solutions, only one short-lived transient species is quantitatively formed, namely $HO\cdot$ radicals, the radiolytic yield of which becoming:

$$G(HO\cdot) = G_{HO\cdot} + G_{e_{aq}-} = 5.6 \times 10^{-7} \text{ mol J}^{-1} \quad (7)$$

The concentration, C, of a radiolytic species produced by water radiolysis can be expressed as a function of the irradiation dose, D, expressed in Grays (1 Gy corresponds to 1 J kg^{-1} or 1 J L^{-1} for diluted solution) according to:

$$C\left(\text{mol L}^{-1}\right) = D\,(\text{Gy}) \times G\left(\text{mol J}^{-1}\right) \quad (8)$$

Then, under N_2 atmosphere in the presence of isopropanol, a dose of 3.6 kGy produces 1 mM in hydrated electrons (and 1 mM in isopropanol radicals), while under N_2O atmosphere, a dose of 1.8 kGy is needed for the production of 1 mM in hydroxyl radicals.

As demonstrated in our previous work (Lattach et al., 2013, 2014), the yield of EDOT monomers oxidation by hydroxyl radicals is strictly equal to the yield of $HO\cdot$ formation. We also demonstrated that the quantitative synthesis of $PEDOT_{ox}$ polymers throughout oxidation–polymerization mechanism implies the use of two $HO\cdot$. radicals per EDOT molecule. This is consistent with the fact that, in a polymer, all the monomers apart from the terminal ones, are bound to two neighbors in α and α′ positions. Thus, the theoretical irradiation dose (D_{max}) which should lead to the quantitative formation of $PEDOT_{ox}$ under N_2O atmosphere is twice the dose necessary for the total oxidation of EDOT monomers. In a N_2O-saturated aqueous solution containing 10 mM in EDOT, due to Eqs. (7) and (8), the dose which is necessary for the total oxidation of EDOT by hydroxyl radicals, amounts to 18 kGy, while the dose D_{max} which is necessary for the complete synthesis of $PEDOT_{ox}$ amounts to 36 kGy.

One can suppose that the quantitative synthesis of $PEDOT_{red}$ polymers throughout reduction–polymerization mechanism implies also the use of two reducing radicals per EDOT molecule. The theoretical irradiation dose (D_{max}) which should lead to the quantitative formation of $PEDOT_{red}$, under N_2 atmosphere in the presence of isopropanol, is then twice the dose necessary for the total reduction of EDOT monomers. Since, isopropanol radicals do not reduce EDOT as it will be further demonstrated and since only hydrated electrons react onto EDOT molecules, due to Eqs. (3) and (8), the doses which are necessary for the total reduction of 1 mM and 10 mM in EDOT, amount to 3.6 and 36 kGy respectively, while the doses D_{max} which are necessary for the complete synthesis of $PEDOT_{red}$, amount to 7.2 and 72 kGy respectively.

2.3. Solutions preparation and γ-irradiation

Aqueous solutions containing different concentrations in EDOT (1 and 10 mM) were prepared at room temperature and in the dark to prevent any photochemical reaction. The chosen EDOT concentrations, which are lower than EDOT solubility in water, was always checked by UV–vis absorption spectroscopy since the spectrum of EDOT had earlier been determined (Lattach et al., 2013). EDOT concentrations higher than 10 mM were not used in order to avoid the direct ionization of EDOT molecules which could occur during radiolysis. The pH of the solutions was, in all the cases, found to be close to 7. Note that no drastic change in the pH was observed after irradiation.

For $PEDOT_{red}$ synthesis, EDOT aqueous solutions were added with isopropanol (0.2 mol L^{-1}), degassed with N_2 for 20 min and then irradiated with increasing doses up to 72 kGy in order to achieve complete polymer synthesis. For comparision purpose and in order to quantitatively synthesize $PEDOT_{ox}$, EDOT aqueous solutions were degassed by bubbling with nitrous oxide, N_2O, for 20 min, in the absence of isopropanol and then irradiated at 72 kGy. All irradiations were carried out with a ^{60}Co panoramic γ-ray source available at LCP laboratory of Paris-Sud University. The γ-ray dose rate was 5 kGy h^{-1} in all cases.

2.4. $PEDOT_{red}$ and $PEDOT_{ox}$ characterization

UV-visible absorption spectra of EDOT (before irradiation) and radiosynthesized $PEDOT_{ox}$ or $PEDOT_{red}$ (after irradiation) solutions were recorded using a HP 8543 spectrophotometer in a quartz cell with an optical path length of 0.2 cm. The reference was water in all cases.

The morphology of $PEDOT_{red}$ in aqueous solution was observed with transmission electron microscopy in a cryogenic environment (cryo-TEM). A drop of each solution was deposited on "quantifoil"® (Quantifoil Micro Tools Gmbh, Germany) 200 mesh holey-carbon-coated grids. After being blotted with filter paper, the grids were quench-frozen by being rapidly plunged into liquid ethane in order to form a thin ice film avoiding water crystallization. The grids were then transferred into the microscope using a side entry Gatan 626 cryoholder cooled at −180 °C with liquid nitrogen. Images were recorded on ultrascan 2k CCD camera (Gatan, USA), using a LaB6 JEOL JEM 2100 (JEOL, Japan) cryo microscope operating at 200 kV with a low dose system (Minimum Dose System, MDS) to protect the thin ice film from any irradiation before imaging and to reduce the irradiation during image capture. By freezing the system, cryo-TEM ensures the observation of soft nano-objects in equilibrium in solution because it avoids the phase transition and possible PEDOT aggregation resulting from drying procedures.

All the solutions of EDOT after γ-irradiation were dried by lyophilization with a Heto PowerDry® LL1500 (Thermo Electron Co., France) to obtain dehydrated powders. The drying procedures were carried out as follows: first, all the solutions were transferred to culture dishes and frozen into ices; then, the frozen samples were moved to the drying chamber and lyophilized at −110 °C for 48 h.

To further identify radiosynthesized polymers and their chemical composition, the Fourier transform infrared (FTIR) spectra of lyophilized $PEDOT_{ox}$ and $PEDOT_{red}$ were recorded using a FTIR spectrometer (Bruker Vertex 70) with diamond ATR attachment (PIKEMIRACLE crystal plate diamond/ZnSe) and MCT detector with a liquid nitrogen cooling system. The lyophilized powders were deposited onto the ZnSe diamond and scanning was conducted from 4000 to 600 cm^{-1} with a 4 cm^{-1} spectral resolution for 100 times and averaged for each spectrum.

In order to check the morphology of radiosynthesized polymers after deposition, $PEDOT_{red}$ powder obtained after lyophilization was sprinkled onto carbon tape adhered to aluminum mounts and the micrographs were obtained with EVO MA 10 tungsten filament Scanning Electron Microscope (SEM). Magnification, accelerating voltage and scale bar were 5 K X, 15 keV and 1 μm.

AFM-IR measurement was carried out by depositing a small drop of $PEDOT_{red}$ solution onto the upper surface of ZnSe prism (transparent in the mid-IR) and dried naturally in air. The dried deposit was observed by nanoIR™ (@Anasys Instruments) an AFM-IR system that combines the AFM with a pulsed infrared OPO laser to perform spectromicroscopy. AFM, which has a visible laser focusing on the cantilever and a four quadrants detector measuring its deflection, was used for the superficial morphology characterization in contact mode. To obtain relevant infrared spectra, the pulsed infrared laser setup covers the wavenumbers from 3600 cm^{-1} to 1000 cm^{-1}. During the measurement, the tip of the

AFM remained in contact with the object. When the sample absorbs an IR laser pulse, the absorbing region warms via the photothermal effect and a rapid thermal expansion occurs which then impacts the tip of the AFM cantilever and causes its oscillation. As the amplitude of oscillations is proportional to the absorption, scanning the surface with a given wavenumber enables the drawing of chemical map of the sample, while changing the wavelength on a fixed position of the tip gives a local infrared spectrum (Dazzi et al., 2005, 2012; Policar et al., 2011).

The thermal stability and composition analysis of lyophilized $PEDOT_{ox}$ and $PEDOT_{red}$ was performed on a thermogravimetric analysis instrument TGA Q500 (TA instruments, USA) under a nitrogen flow of 50 mL/min. The temperature ranged from 40 to 900 °C at a heating rate of 20 °C/min.

To measure the conductivity of $PEDOT_{ox}$ and $PEDOT_{red}$, spin-coated films of PEDOT were obtained by spinning a small drop of PEDOT suspensions on an ITO substrate. Before measurements, the nanostructures of PEDOT solutions or suspensions were doped with $NOBF_4$ at a concentration of 10 mM in acetonitrile. A Kelvin four-point probe technique was used for measuring the resistance of $PEDOT_{ox}$ and $PEDOT_{red}$ films and a 3 Veeco Dektak 150 surface profiler was used for the thickness measurement of the films. The conductivity, ρ (S cm^{-1}) was determined thanks to the following equation:

$$\rho = \left(\frac{\pi}{\ln 2} \times \frac{V}{I} \times t\right)^{-1} \tag{9}$$

where V is the voltage difference (V), t is the film thickness (cm) and I is the applied current (A).

3. Results and discussion

3.1. Hydrated electrons-induced EDOT reduction

In a previous work, we already demonstrated that, at air and under N_2O atmosphere, hydroxyl radicals quantitatively oxidize EDOT molecules (Lattach et al., 2013, 2014), the yield of EDOT monomers oxidation being strictly equal to the yield of formation of HO· radicals. In order to check whether EDOT molecules can be alternatively reduced by radical species produced by water radiolysis, we irradiated aqueous solutions containing 1 mM in EDOT at increasing doses up to 7.2 kGy under N_2 in the presence of 0.2 mol L^{-1} isopropanol.

The UV–vis absorption spectrum of aqueous solution containing 1 mM in EDOT displays two absorption maxima at 235 and 255 nm as shown in Fig. 1. The characteristic peak of EDOT monomers at 255 nm arises from $\pi \rightarrow \pi^*$ electronic transitions in the thiophene ring and its extinction coefficient value was estimated to be 7048 L mol^{-1} cm^{-1} (Lattach et al., 2013). The evolution of the UV–visible absorption spectrum of this solution as a function of the irradiation dose displays a continuous decrease in the absorption at 235 and 255 nm (results not shown) indicating the progressive consumption of EDOT (according to a pseudo-first-order exponential decay). From the value of the extinction coefficients at 255 nm, we deduced the variation in EDOT concentration with the irradiation dose (Inset of Fig. 1). The initial radiolytic yield of EDOT consumption, $G_{-EDOT\ 0}$, is given by the value of the initial slope of the curve which can be deduced thanks to an exponential fit of the experimental curve:

$$G_{-EDOT\ 0}(\text{mol J}^{-1}) = -\left(\frac{d[\text{EDOT}]\ (\text{mol L}^{-1})}{\text{dDose (Gy)}}\right)_0 = 2.6 \times 10^{-7}\ \text{mol J}^{-1} \tag{10}$$

The same yield is obtained when irradiations are performed in the presence of tert-butanol (instead of isopropanol) which is also a scavenger of HO· radicals. Nevertheless, contrarily to isopropanol radicals, tert-butanol radicals are known to be unreactive. These results demonstrate that, under N_2 in the presence of isopropanol, only hydrated electrons react with EDOT monomers. In addition, we clearly find that:

$$G_{-EDOT\ 0} \sim G_{e_{aq}^-} \tag{11}$$

This indicates that a concentration of 1 mM in EDOT is sufficient to scavenge all the hydrated electrons produced by radiolysis of water and that e_{aq}^- quantitatively reduce EDOT monomers.

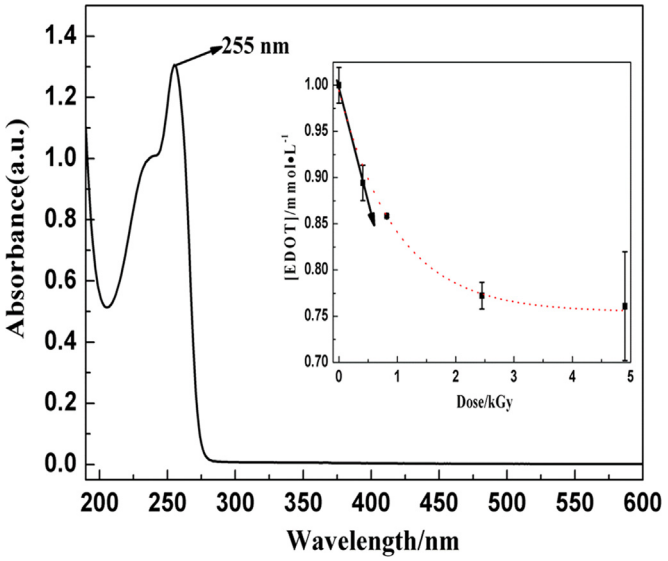

Fig. 1. Absorption spectrum of an aqueous solution containing 1 mM in EDOT. The optical path length was 0.2 cm. The reference was water. Inset: variation of EDOT concentration as a function of the dose. The initial radiolytic yield of EDOT consumption corresponds to the initial slope of the curve.

3.2. Radiation-induced reduction–polymerization of EDOT

In a previous work, we demonstrated that, at air and under N_2O atmosphere, HO·-induced oxidation of EDOT implies the formation of a transient species, namely $EDOT^{\cdot +}$ cation radical, which dimerizes and deprotonates leading to a stable product, namely $EDOT_2$ dimer (Coletta et al., 2015). This result proves that $PEDOT_{ox}$ growth is not a chain reaction. On the contrary, it proceeds through a step-by-step mechanism made up of the following recurrent steps: (i) oxidation/activation, (ii) growth/chain length increase, (iii) deprotonation. As a consequence, $PEDOT_{ox}$ radio-induced synthesis proceeds through a recurrent oxidation process: HO· reacts with EDOT monomers, then with dimers, then with oligomers… This means that the quantitative synthesis of $PEDOT_{ox}$ polymers throughout oxidation–polymerization mechanism implies the use of two HO·. radicals per EDOT molecule. This has also been demonstrated (Lattach et al., 2013, 2014) since doses higher than 36 kGy enabled the quantitative radiation-induced oxidation polymerization of 10 mM in EDOT under N_2O atmosphere.

While hydroxyl radicals oxidize EDOT monomers leading to $PEDOT_{ox}$ polymers, hydrated electrons are able to reduce EDOT and, by comparison, should lead to $PEDOT_{red}$ polymers. The fact that the yield of EDOT consumption is equal to that of e_{aq}^- production (Eq. (11)) means that the process initiated by hydrated electrons and which will be further attributed to $PEDOT_{red}$ radio-induced synthesis does not proceed through a chain reaction. Then, one can suppose that the quantitative synthesis of $PEDOT_{red}$ polymers throughout a reduction–polymerization process implies

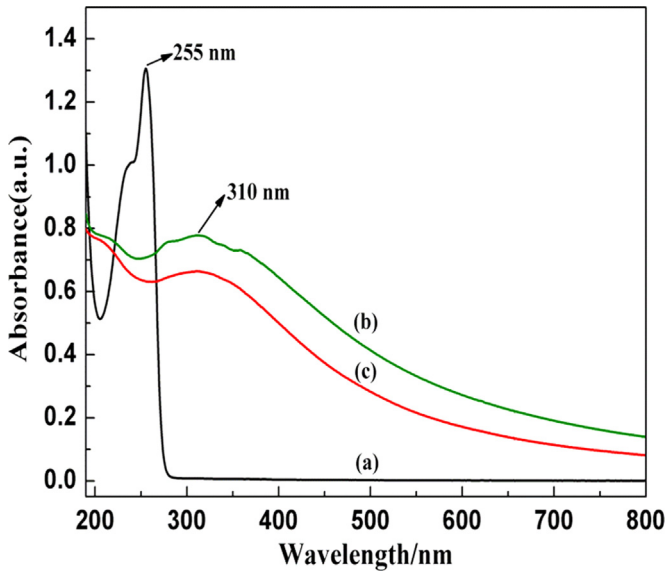

Fig. 2. Absorption spectra of an aqueous solution containing 10 mM in EDOT (a) before irradiation, (b) irradiated at 72 kGy under N_2 in the presence of isopropanol ($PEDOT_{red}$), (c) irradiated at 72 kGy under N_2O ($PEDOT_{ox}$). The optical path length was 0.2 cm. The reference was water.

also a step-by-step mechanism and then needs the use of two hydrated electrons per EDOT molecule.

In order to check whether reduction of EDOT monomers by e^-_{aq} is accompanied by a radiation-induced polymerization process, we irradiated, under N_2 in the presence of 0.2 mol L^{-1} isopropanol, aqueous solutions containing 10 mM in EDOT at increasing doses up to 72 kGy (Fig. 2, spectrum b). This used dose is that needed for the total reduction of EDOT in case of a step-by step reduction–polymerization mechanism. Note that while low concentrations in EDOT monomers (1 mM) were needed for succeeding in the follow-up of their reduction mechanism, higher concentrations in EDOT were necessary for the characterization of $PEDOT_{red}$ polymers, either in aqueous solution or after their deposition onto substrate as it will be further presented in the case of 10 mM in EDOT.

In Fig. 2, the UV–visible absorption spectrum of the solution irradiated (at 72 kGy) under N_2 in the presence of isopropanol (spectrum b) is similar to the spectrum we previously obtained for $PEDOT_{ox}$ (at the same dose) under N_2O (spectrum c, Lattach et al., 2014). Only a small difference between the intensities of the spectra is observed. In both cases, the two absorption bands of EDOT monomers at 235 and 255 nm (spectrum a) have completely disappeared, which should indicate that oxidation–polymerization as well as reduction–polymerization are quantitative at 72 kGy (D_{max}) as expected. Both spectra display an absorption maximum around 310 nm, which has previously been attributable to EDOT dimers and oligomers (Tran-Van et al., 2001; Hulvat and Stupp, 2004). Such a band was also observed in our previous work in the case of oxidation–polymerization (Lattach et al., 2014). Also, spectra are characterized by a continuous scattering in the range of 400–800 nm which should correspond to longer oligomers and polymers of PEDOT (Hohnholz et al., 2001; Zhao et al., 2014; Han and Foulger, 2006). The observed light scattering traduces the presence in the irradiated solutions of a dense yellow suspension such as that observed in Fig. 3 (photography b) in the case of EDOT solution irradiated under N_2. As it will be later demonstrated thanks to ATR-FTIR spectroscopic measurements, these suspensions correspond to $PEDOT_{red}$ and $PEDOT_{ox}$ polymers formed at high doses thanks respectively to the reduction–polymerization and the oxidation–polymerization processes.

3.3. *Highlighting $PEDOT_{red}$ radioinduced synthesis*

After a 72 kGy-irradiation under N_2, the original transparent aqueous solution of EDOT monomers in the presence of isopropanol (Fig. 3, photo a) becomes turbid (Fig. 3, photo b). The yellow suspension was then dried by lyophilization in order to eliminate any residual water molecules which could be trapped in the polymer-containing dark solid phase obtained (Fig. 3, photo c). For comparison, EDOT aqueous solution irradiated at 72 kGy under N_2O was also lyophilized. The lyophilized samples were then characterized by ATR-FTIR spectroscopy in order to investigate the chemical nature of the solid phases and to confirm the presence of PEDOT polymers in both of them.

The ATR-FTIR spectra of both powders, radiosynthesized at 72 kGy under reducing (spectrum b) and oxidizing conditions (spectrum c), are presented in Fig. 4 in the wave number region 4000–600 cm^{-1} together with the spectrum of pure non irradiated EDOT (spectrum a). Between 1600 and 600 cm^{-1}, the three obtained spectra are in good agreement with those previously reported for PEDOT and EDOT in literature. The absorption bands at 890, 1054 and 1182 cm^{-1} correspond to the stretching vibrations of ethylenedioxy group (C–O–R–O–C). The stretching vibrations of C–C and C=C in thiophene ring are also observed at 1365 and 1481 cm^{-1} (Kvarnström et al., 1999). The absorption bands at 1361, 1430 and 1488 cm^{-1} originating from C–C and C=C (Tran-Van et al., 2001) can be seen in the ATR-FTIR spectra of both powders. All the characteristic bands of PEDOT are then present in spectra b and c of Fig. 4 even if they appear relatively slightly displaced. For instance, the absorption band assigned to ethylenedioxy group is observed at 1087 cm^{-1} in the case of the powder obtained by reduction–polymerization, while it appears at 1064 cm^{-1} in the case of the powder obtained by oxidation. Nevertheless, this demonstrates, without any ambiguity, that PEDOT polymers are obtained by radiolysis either by reduction–polymerization or by oxidation–polymerization.

Note that the characteristic peak at 755 cm^{-1}, attributed to the C–H out-of-plane bending vibration at α, α′ positions of EDOT (spectrum a), totally disappears after irradiation (spectra b and c).

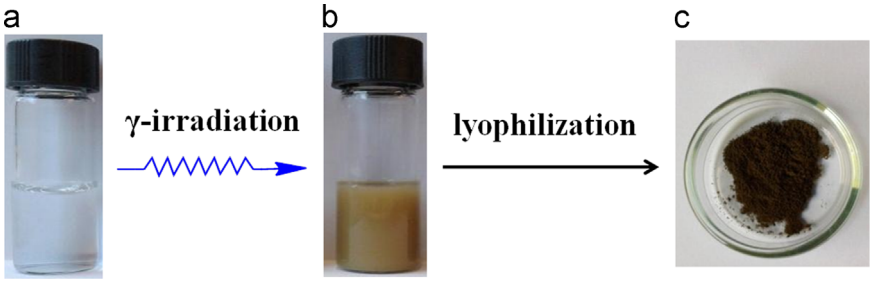

Fig. 3. Photographs of EDOT samples (a) at a concentration of 10 mM before irradiation, (b) after a 72 kGy-irradiation under N_2 in the presence of isopropanol ($PEDOT_{red}$), (c) after lyophilization.

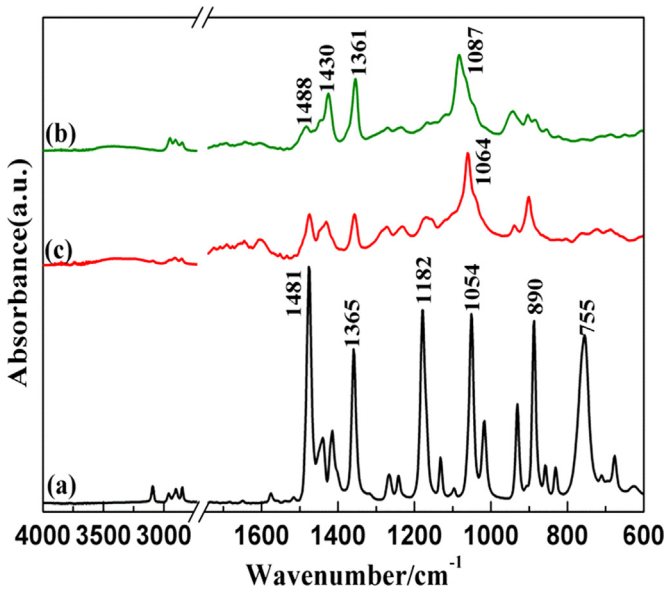

Fig. 4. ATR-FTIR spectra of (a) pure EDOT monomers, (b) $PEDOT_{red}$ powder obtained by reduction–polymerization at 72 kGy, (c) $PEDOT_{ox}$ powder obtained by oxidation–polymerization at 72 kGy.

This result proves the successful synthesis of $PEDOT_{red}$ and $PEDOT_{ox}$ via α, α′ coupling reactions (Lattach et al., 2014) and definitely demonstrates that EDOT polymerization is complete at 72 kGy, in agreement with a step-by-step PEDOT growth mechanism in both oxidizing and reducing conditions.

3.4. *Morphological characterization of $PEDOT_{red}$*

Aqueous solutions containing 10 mM in EDOT and irradiated at 72 kGy under N_2 in the presence of isopropanol were observed by cryo-transmission electron microscopy just after irradiation and before any sedimentation. Representative images showed the presence of low density globular structures forming polydisperse spherical nanoparticles with a diameter comprised between 100 and 500 nm as observed on Fig. 5 (images a and b at two different magnifications). Since no other low density objects were observed during our cryo-TEM experiments, we deduce that these spherical nanoparticles are made up of $PEDOT_{red}$ polymers.

The mean size, the shape and the polydispersity of $PEDOT_{red}$ polymer nanostructures obtained in the present work, through reduction–polymerization, are the same as those of $PEDOT_{ox}$ polymers already synthesized through oxidation–polymerization routes induced either by γ-rays (Lattach et al., 2013, 2014) or by accelerated electrons (Coletta et al., 2015).

Each observed nanoparticle should be composed of interdigitated polymer chains. Since no parasite α – β′ linkages could occur during polymerization, radiosynthesized $PEDOT_{red}$ nanostructures must be composed of linear chain polymers which are not branched nor networked. Thus, each globular structure observed on Fig. 5 should correspond to a self-assembly of independent amorphous PEDOT chains.

In order to characterize the morphology of the polymers after drying and deposition procedures, $PEDOT_{red}$-containing lyophilized powder obtained after a 72 kGy-irradiation was deposited onto carbon tape adhered to aluminum mounts and dried. The surface was then imaged by Scanning Electron Microscopy. The images of Fig. 6, displayed at two different magnifications (images a and b), indicate the presence of very close-packed spheroid polymeric particles. These structures should come from the globular nanostructures already observed in aqueous solution by cryo-TEM (Fig. 5). All these observations are consistent with the reported characterizations of $PEDOT_{ox}$ polymers synthesized by oxidation–polymerization (Lattach et al., 2014). The particles observed by SEM after deposition are polydisperse in size with a diameter comprised between 100 and 500 nm. These SEM observations agree well with the morphology of $PEDOT_{red}$ particles previously observed in aqueous solution by Cryo-TEM (Fig. 5) without any significant change in the mean size and in the shape. Then, the packing of the particles and their flattening onto the substrate when deposited and dried do not seem to affect the nanostructuration of $PEDOT_{red}$ polymers.

In order to further prove that the spherical nanoparticles already observed by cryo-TEM and SEM are made up of PEDOT polymer chains, a drop of the yellow suspension (Fig. 3, photo b, obtained after the irradiation at 72 kGy of an aqueous solution containing 10 mM in EDOT under N_2 in the presence of isopropanol) was deposited on the upper surface of a ZnSe prism, dried naturally and finally imaged and characterized by AFM-IR (Fig. 7).

According to the AFM image of $PEDOT_{red}$ recorded in contact mode (Fig. 7a), the bottom dark areas having no thickness correspond to the substrate. The topography of $PEDOT_{red}$ displayed as the bright areas correspond to the thicker regions made up of close-packed spherical nanoparticles (100–300 nm in diameter). This AFM observation agrees well with the morphology of $PEDOT_{red}$ globular particles previously observed in aqueous solution by Cryo-TEM (Fig. 5) without any significant change in the mean size and in the

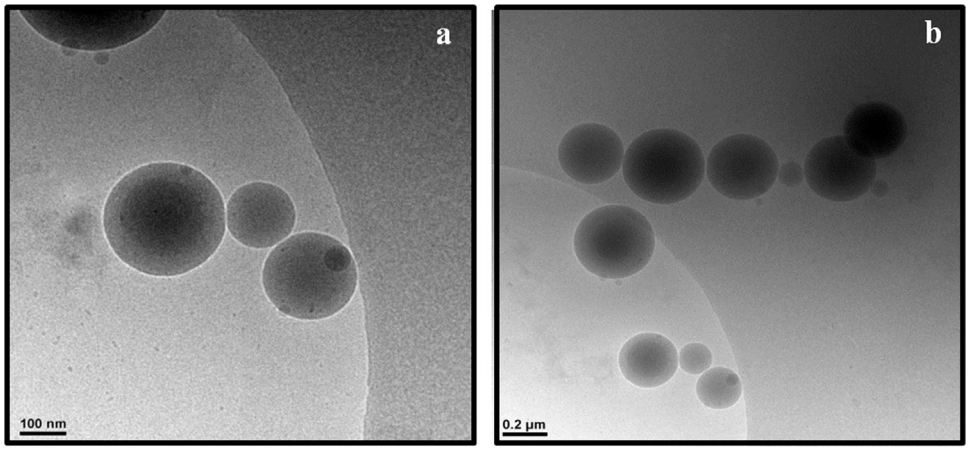

Fig. 5. Cryo-TEM images of aqueous samples containing 10 mM in EDOT irradiated at 72 kGy under N_2 in the presence of isopropanol. They exhibit spherical nanoobjects with diameters comprised between 100 and 500 nm attributed to self-assembled $PEDOT_{red}$ polymers.

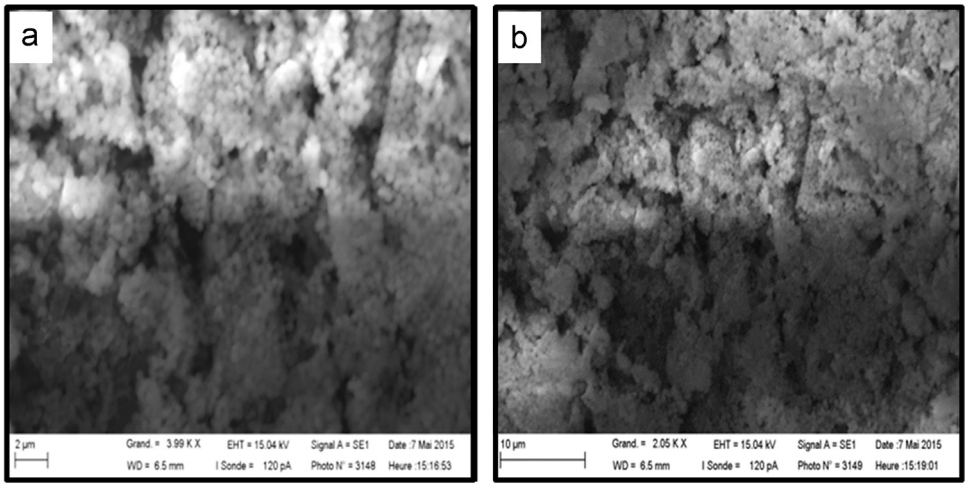

Fig. 6. SEM images of $PEDOT_{red}$ polymers after lyophilization and deposition onto carbon tape adhered to aluminum mounts. Polymers were obtained after a 72 kGy-irradiation of an aqueous solution containing 10 mM in EDOT under N_2 in the presence of isopropanol.

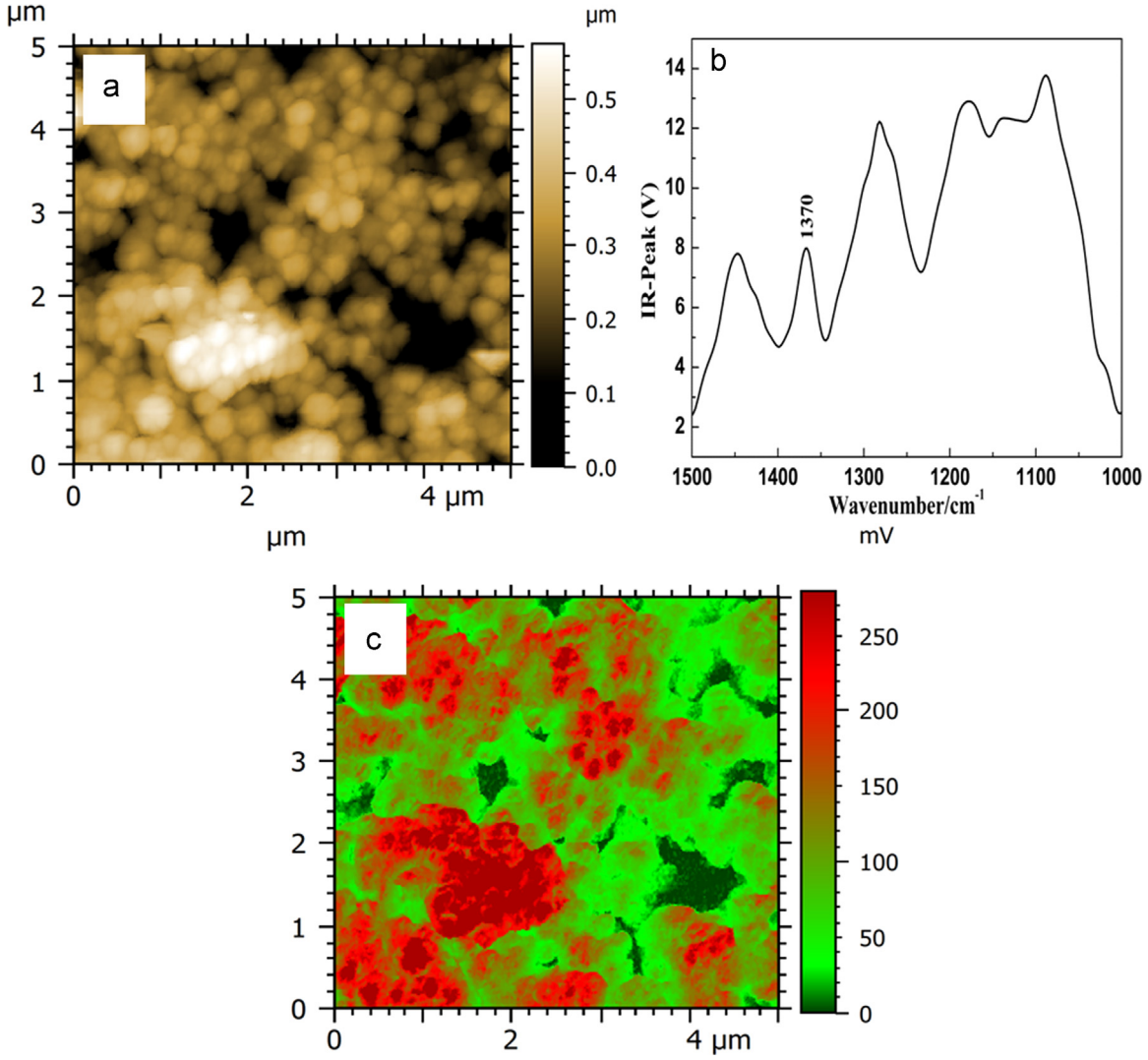

Fig. 7. AFM-IR characterization of PEDOT polymers synthesized according to reduction–polymerization (a) AFM topographic image of $PEDOT_{red}$ polymers in contact mode, (b) AFM-IR spectrum of $PEDOT_{red}$ polymers and (c) AFM-IR chemical mapping of $PEDOT_{red}$ polymers with the IR source tuned to the C–C band at 1370 cm^{-1}. Samples containing 10 mM in EDOT were irradiated at 72 kGy under N_2 in the presence of isopropanol, then deposited onto ZnSe prism after lyophilisation. (For interpretation of the references to color in this figure, the reader is referred to the web version of this article.)

shape. Then, the packing of the particles and their flattening onto ZnSe substrate when deposited and dried do not seem to affect the nanostructuration of polymer nanostructures.

In order to confirm that these nanoparticles are made up of PEDOT polymers, the sample was observed by AFM-IR in the range of 1000–1500 cm^{-1} (Fig. 7b). The spectrum of Fig. 7b displays a peak at 1370 cm^{-1} which corresponds to the C–C stretching band of PEDOT as observed in ATR-FTIR spectra at 1361 cm^{-1} (Fig. 4, spectrum b). This definitely demonstrates that the nanoparticles observed in Fig. 7a, and also in Figs. 5 and 6, contain close-packed $PEDOT_{red}$ polymer chains.

Since the AFM-IR technique also enables the chemical mapping of the sample, this wavenumber 1370 cm^{-1} was chosen for AFM-IR chemical mapping of our sample. The chemical map was scanned and the absorption strength was recorded. (Fig. 7c). In Fig. 7c, the red areas indicate a stronger absorption at the characteristic wavenumber which is caused by a thick layer of $PEDOT_{red}$ (~300 nm) linked onto the prism. When comparing the topography (Fig. 7a) and the chemical mapping (Fig. 7c), one can observe that the stronger absorbing areas fit very well with the thicker regions, which implies that the spherical nanoparticles are mainly composed by PEDOT polymer chains (Ghosh et al., 2014). Therefore, we conclude, without any ambiguity that radiation chemistry in reducing conditions (in the presence of hydrated electrons) leads to the reduction of EDOT monomers and to the growth of PEDOT polymers which self-assemble into spherical nanoparticles (of few hundred nanometers in diameter), those we observed in this work by cryo-TEM, SEM and AFM (Figs. 5, 6 and 7 respectively).

3.5. *Physicochemical properties of $PEDOT_{red}$, a comparison with those of $PEDOT_{ox}$*

We wanted to check and to compare the thermal stability of $PEDOT_{red}$ and $PEDOT_{ox}$ previously synthesized (under reducing conditions and oxidative conditions, respectively) and obtained as powders after lyophilization. The thermogravimetric analysis (TGA) plots of both polymers are displayed in Fig. 8. The degradation curves (green lines), which indicate the remaining weight of PEDOT powders as a function of temperature, are represented together with the weight derivative curves (red lines).

In the case of $PEDOT_{red}$ (Fig. 8a), it can be found that a slow weight loss takes place before 150 °C due to the evaporation of water and the degradation of PEDOT oligomers (Nagarajan et al., 2008). Then, a continuous decomposition occurs between 250 and 450 °C due to PEDOT fragmentation and carbon oxidation. This decomposition results in about a 70% weight lost. The quick degradation observed with temperature may be caused by the relatively small PEDOT particles size. Indeed, smaller particles are characterized by higher surface area for heat transfer (Paradee and Sirivat, 2014). After 450 °C, weight loss of residuals is negligible. For comparison purpose, the TGA curve of $PEDOT_{ox}$ was also recorded (Fig. 8b) and the degradation processes are quite similar for both PEDOT synthesized by reduction–polymerization and oxidation–polymerization. The present results, which are in good agreement with earlier reports on PEDOT polymers (Feng et al., 2013), indicate that $PEDOT_{red}$ is characterized by a good thermal stability, at least comparable to that of PEDOT polymers usually synthesized by oxidative routes.

At the end, we wanted to check and to compare the electrical conductivity of $PEDOT_{red}$ and $PEDOT_{ox}$ (synthesized under reducing conditions and oxidative conditions, respectively) by four point probe technique. In this aim, we doped both samples with $NOBF_4$ (10 mM). The average electrical conductivity of $PEDOT_{red}$ was found to be 3.4×10^{-3} S cm^{-1}. This value is close to PEDOT conductivity values already reported in literature (Nagarajan et al., 2008; Jones et al., 2012). We thus succeeded in the synthesis of conducting materials thanks to our original radiation-induced reduction–polymerization route. Nevertheless, we can note that $PEDOT_{red}$ conductivity, which has not been optimized yet, remains somewhat lower than that of $PEDOT_{ox}$ polymers, which amounts to 9.8×10^{-3} S cm^{-1}.

4. Conclusion

Current research aims to develop new synthesis strategies and new conducting polymers with tuned morphologies and properties. We recently, and for the first time in literature, succeeded in the development of a new radiolysis-based alternative methodology for synthesizing conducting polymers in aqueous solution. High energy γ-rays (Lattach et al., 2013, 2014; Cui et al., 2014) as well as high energy electrons irradiator (Coletta et al., 2015) were successfully used to generate oxidizing species, namely hydroxyl

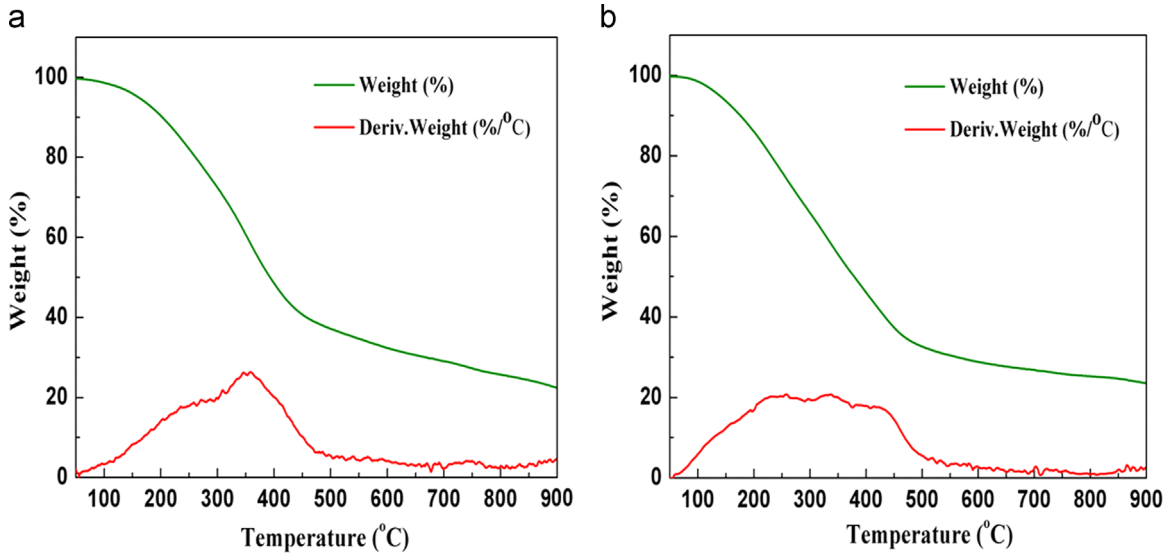

Fig. 8. Thermogravimetric analysis (TGA) plots and weight derivative curves of (a) $PEDOT_{red}$ polymers synthesized under N_2 in the presence of isopropanol with a 72 kGy-irradiation, (b) $PEDOT_{ox}$ polymers synthesized under N_2O with a 72 kGy-irradiation. (For interpretation of the references to color in this figure legend, the reader is referred to the web version of this article.)

radicals, through water radiolysis, inducing first oxidation of monomers and then polymers growth. This radiation-induced oxidation–polymerization route, which has been shown to proceed through a step by step oxidation process, enabled the preparation of nanostructured PEDOT ($PEDOT_{ox}$) and PPy conducting polymers.

In the present paper, radiolysis was used, in a different way, to generate reducing species (instead of oxidizing radicals), namely hydrated electrons, in order to reduce monomers and to induce polymers growth. Starting from EDOT monomers dissolved in water, we describe for the first time this simple γ-rays-based reduction–polymerization route for synthesizing PEDOT conducting polymers in aqueous solution ($PEDOT_{red}$).

$PEDOT_{red}$ polymers synthesized by radiation-induced reduction polymerization are characterized by a very good long-term stability at air in a humid environment. We showed that the as-prepared $PEDOT_{red}$ polymers remain well dispersed in water, can be easily dried and are quite simply redispersed in protic solvents. The chemical nature of $PEDOT_{red}$ polymers was confirmed by ATR-FTIR spectroscopy while their morphology was checked in solution by cryo-TEM microscopy and after lyophilisation and deposition by SEM microscopy and AFM-IR nanospectroscopy. $PEDOT_{red}$ polymers were found to form polydisperse spherical nanoparticles whose morphology was kept after deposition onto solid substrates. Finally, the electrical conductivity of $PEDOT_{red}$ was evaluated at $3.4 \times 10^{-3}\ S\ cm^{-1}$. This conductivity is comparable to conductivities already reported in literature concerning PEDOT polymers synthesized by conventional oxidative methodologies, but remains somewhat lower than that of $PEDOT_{ox}$ polymers we previously synthesized by oxidation–polymerization.

Work is in due course in order to enhance the conductivity of $PEDOT_{red}$ and $PEDOT_{ox}$ polymers by the way of the improvement of their doping level and thanks to the increase in their conjugation length. Also, in order to control the growth and the morphology of radiosynthesized $PEDOT_{red}$ and $PEDOT_{ox}$ polymers, soft templates such as hexagonal mesophases or spherical micelles will be used.

Finally, the study of the influence of polymerization mechanism remains poorly investigated in literature in the field of conducting materials. We thus aim to progress in this domain in order to find out the better way to optimize the preparation of nanostructured conducting polymers with adjusted morphologies and tuned properties. We already used pulse radiolysis in order to study hydroxyl radicals-induced EDOT oxidation and to determine the oxidation–polymerization mechanism which leads to $PEDOT_{ox}$ conducting polymers. Such fast kinetic studies are underway in order to identify the first steps of hydrated electrons-induced reduction–polymerization mechanism and in order to better understand the growth process of $PEDOT_{red}$ polymers in aqueous solution.

Acknowledgments

We acknowledge the financial support from the China Scholarship Council (CSC). Also, we thank Jean-Michel Guigner (IMPMC, UMR 7590, CNRS, Université Pierre et Marie Curie, France) for Cryo-TEM experiments.

References

Abdelhamid, M.E., O'Mullane, A.P., Snook, G.A., 2015. Storing energy in plastics: a review on conducting polymers & their role in electrochemical energy storage. RSC Adv. 5, 11611–11626.

Adeloju, S.B., Wallace, G.G., 1996. Conducting polymers and the bioanalytical sciences: new tools for biomolecular communications. Analyst 121, 699–703.

Atanasov, S.E., Losego, M.D., Gong, B., Sachet, E., Maria, J.P., Williams, P.S., Parsons, G.N., 2014. Highly conductive and conformal poly(3,4-ethylenedioxythiophene) (PEDOT) thin films via oxidative molecular layer deposition. Chem. Mater. 26, 3471–3478.

Baik, W., Luan, W.Q., Zhao, R.H., Koo, S., Kim, K.S., 2009. Synthesis of highly conductive poly(3,4-ethylenedioxythiophene) fiber by simple chemical polymerization. Synth. Met. 159, 1244–1246.

Balint, R., Cassidy, N.J., Cartmell, S.H., 2014. Conductive polymers: towards a smart biomaterial for tissue engineering. Acta Biomater. 10, 2341–2353.

Belloni, J., Mostafavi, M., Remita, H., Marignier, J.L., Delcourt, M.O., 1998. Radiation-induced synthesis of mono- and multi-metallic clusters and nanocolloids. New J. Chem., 1239–1255.

Cho, B., Park, K.S., Baek, J., Oh, H.S., Koo Lee, Y.E., Sung, M.M., 2014. Single-crystal poly(3,4-ethylenedioxythiophene) nanowires with ultrahigh conductivity. Nano Lett. 14, 3321–3327.

Coletta, C., Cui, Z., Archirel, P., Pernot, P., Marignier, J.L., Remita, S., 2015. Electron-induced growth mechanism of conducting polymers: a coupled experimental and computational investigation. J. Phys. Chem. B 119, 5282–5298.

Cui, Z., Coletta, C., Dazzi, A., Lefrancois, P., Gervais, M., Neron, S., Remita, S., 2014. Radiolytic method as a novel approach for the synthesis of nanostructured conducting polypyrrole. Langmuir 30, 14086–14094.

Dazzi, A., Prazeres, R., Glotin, F., Ortega, J.M., 2005. Local infrared microspectroscopy with subwavelength spatial resolution with an atomic force microscope tip used as a photothermal sensor. Opt. Lett. 30, 2388–2390.

Dazzi, A., Prater, C.B., Hu, Q.C., Bruce Chase, D., Rabolt, J.,F., Marcott, C., 2012. AFM–IR: combining atomic force microscopy and infrared spectroscopy for nanoscale chemical characterization. Appl. Spectrosc. 66, 1365–1384.

Feng, Z.Q., Wu, J., Cho, W., Leach, M.K., Franz, E.W., Naim, Y.I., Gu, Z.Z., Corey, J.M., Martin, D.C., 2013. Highly aligned poly(3,4-ethylene dioxythiophene) (pedot) nano- and microscale fibers and tubes. Polymer 54, 702–708.

Ferradini, C., Jay-Gerin, J.P., 1999. Radiolysis of water and aqueous solutions-history and present state of the science. Can. J. Chem. 77, 1542–1575.

Ferradini, C., Jay-Gerin, J.P., 2000. The effect of pH on water radiolysis: a still open question-a minireview. Res. Chem. Intermed. 26, 549–565.

Ghosh, S., Remita, H., Ramos, L., Dazzi, A., Deniset-Besseau, A., Beaunier, P., Goubard, F., Aubert, P.H., Brisset, F., Remita, S., 2014. PEDOT nanostructures synthesized in hexagonal mesophases. New J. Chem. 38, 1106–1115.

Ghosh, S., Kouamé, N.A., Ramos, L., Remita, S., Dazzi, A., Deniset-Besseau, A., Beaunier, P., Goubard, F., Aubert, P.H., Remita, H., 2015. Conducting polymer nanostructures for photocatalysis under visible light. Nat. Mater. 14, 505–511.

Han, M.G., Foulger, S.H., 2006. Facile synthesis of poly(3,4-ethylenedioxythiophene) nanofibers from an aqueous surfactant solution. Small 2, 1164–1169.

Hart, E.J., 1969. Research potentials of the hydrated electron. Acc. Chem. Res. 2, 161–167.

Heeger, A.J., 2001. Semiconducting and metallic polymers: the fourth generation of polymeric materials (nobel lecture). Angew. Chem. Int. Ed. 40, 2591–2611.

Hohnholz, D., MacDiarmid, A.G., Sarno, D.M., Jones, J.W.E., 2001. Uniform thin films of poly-3,4-ethylenedioxythiophene (PEDOT) prepared by in-situ deposition. Chem. Commun., 2444–2445.

Hulvat, J.F., Stupp, S.I., 2004. Anisotropic properties of conducting polymers prepared by liquid crystal templating. Adv. Mater. 16, 589–592.

Jang, J., Chang, M., Yoon, H., 2005. Chemical sensors based on highlyconductive poly (3,4-ethylene-dioxythiophene) nanorods. Adv. Mater. 17, 1616–1620.

Jiang, C.Q., Chen, G.M., Wang, X., 2012. High-conversion synthesis of poly(3,4-ethylenedioxythiophene) by chemical oxidative polymerization. Synth. Met. 162, 1968–1971.

Jones, B.H., Cheng, K.Y., Holmes, R.J., Lodge, T.P., 2012. Nanoporous poly(3,4-ethylenedioxythiophene) derived from polymeric bicontinuous microemulsion templates. Macromolecules 45, 599–601.

Kirchmeyer, S., Reuter, K., 2005. Scientific importance, properties and growing applications of poly(3,4-ethylenedioxythiophene). J. Mater. Chem. 15, 2077–2088.

Kvarnström, C., Neugebauer, H., Blomquist, S., Ahonenc, H.J., Kankarec, J., Ivaska, A., 1999. In situ spectroelectrochemical characterization of poly(3,4-ethylenedioxythiophene). Electrochim. Acta 44, 273–2750.

Lattach, Y., Deniset-Besseau, A., Guigner, J.M., Remita, S., 2013. Radiation chemistry as an alternative way for the synthesis of PEDOT conducting polymers under "soft" conditions. Radiat. Phys. Chem. 82, 44–53.

Lattach, Y., Coletta, C., Ghosh, S., Remita, S., 2014. Radiation-induced synthesis of nanostructured conjugated polymers in aqueous solution: fundamental effect of oxidizing species. Chemphyschem 15, 208–218.

Lawal, A.T., Wallace, G.G., 2014. Vapour phase polymerisation of conducting and non-conducting polymers: a review. Talanta 119, 133–143.

Li, C., Bai, H., Shi, G., 2009. Conducting polymer nanomaterials: electrosynthesis and applications. Chem. Soc. Rev. 38, 2397–2409.

Nagarajan, R., Kumar, J., Bruno, F.F., Samuelson, L.A., Nagarajan, R., 2008. Biocatalytically synthesized poly(3,4-ethylenedioxythiophene). Macromolecules 41, 3049–3052.

Paradee, N., Sirivat, A., 2014. Synthesis of poly(3,4-ethylenedioxythiophene) nanoparticles via chemical oxidation polymerization. Polym. Int. 63, 106–113.

Patil, A.O., Heeger, A.J., Wudl, F., 1988. Optical properties of conducting polymers. Chem. Rev. 88, 183–200.

Policar, C., Waern, J.B., Plamont, M.A., Clede, S., Mayet, C., Prazeres, R., Ortega, J.M., Vessieres, A., Dazzi, A., 2011. Subcellular IR imaging of a metal–carbonyl moiety using photothermally induced resonance. Angew. Chem. Int. Ed. 50, 860–864.

Roncali, J., Blanchard, P., Frère, P., 2005. 3,4-Ethylenedioxythiophene (EDOT) as a versatile building block for advanced functional π-conjugated systems. J. Mater. Chem. 15, 1589–1610.
Rumbau, V., Pomposo, J.A., Eleta, A., Rodriguez, J., Grande, H., Mecerreyes, D., Ochoteco, E., 2007. First enzymatic synthesis of water-soluble conducting poly (3,4-ethylenedioxythiophene). Biomacromolecules 2, 315–317.
Song, L.Y., Wang, M.Z., Cong, Y.H., Liu, W.J., Ge, X.W., Zhang, Z.C., 2007. The mechanism of 60Co γ-ray radiation induced interfacial redox reaction in inverse emulsion and its application in the synthesis of polymer microcapsules. Polymer 48, 150–157.
Spinks, J.W.T., Woods, R.J., 1990. An Introduction to Radiation Chemistry. 3. John Wiley & Sons, Inc., New York, United States, pp. 251–256.
Tran-Van, F., Garreau, S., Louarn, G., Froyer, G., Chevrot, C., 2001. Fully undoped and soluble oligo(3,4-ethylenedioxythiophene)s: spectroscopic study and electrochemical characterization. J. Mater. Chem. 11, 1378–1382.
Wang, Y., 2009. Research progress on a novel conductive polymer–poly(3,4-ethylenedioxythiophene) (PEDOT). JPCS 152, 012023.
Zhao, Q., Jamal, R., Zhang, L., Wang, M.C., Abdiryim, T., 2014. The structure and properties of PEDOT synthesized by template-free solution method. Nanoscale Res. Lett. 9, 557.